Spectral Simulation of the ESR Spectra of Polyphenol Radicals Formed by Reaction with Hydroxyl Radical

Hisashi Yoshioka,*,† Yasunori Ohashi,‡ Hiroshi Fukuda,§ Yasushi Senba,† and Hiroe Yoshioka‡

Institute for Environmental Sciences and School of Administration and Informatics, University of Shizuoka, 52-1 Yada, Shizuoka-shi 422-8526, Japan, and Radiochemistry Research Laboratory, Faculty of Science, Shizuoka University, 836 Ohya, Shizuoka-shi 422-8529, Japan

Received: September 6, 2002; In Final Form: December 11, 2002

ESR spectra of the short-lived radicals of catechol and gallic acid formed by reaction with hydroxyl radical ($HO^{\bullet}$) in acidic solution were measured using a dielectric mixing resonator and were compared with those formed by autoxidation in an alkaline solution. The triple triplet and triplet absorptions of catechol and gallic acid in alkaline solution showed that they were the phenoxy radicals and that the residual phenolic hydroxyl groups (ϕ-OH) were ionized. On the contrary, the lines were broad and unresolvable in acidic solution, suggesting that the radicals were exchanging between some limiting structures with a rate that affected the line shape. The radical is thought to be phenoxy formed by dehydrogenation with $HO^{\bullet}$, and the position of the unpaired electron can move to another ϕ-OH through a cationic radical structure as an intermediate. Thus, a simulation was performed assuming that the Bloch equation is applicable to some groups of the lines of the limiting structures. A method for the quantum-chemical analysis was developed, and the exchange rate and the hyperfine splitting constants were obtained from the best-fit spectra using a revised Marquardt method. The results suggest that polyphenols scavenge $HO^{\bullet}$ using the ϕ-OHs, but it was impossible to determine which ϕ-OH was used from the ESR spectra because the structure was changing among a few structures.

Introduction

Green tea catechins show various pharmacological activities such as anticarcinogenic,[1] antimutagenic,[2] and antibacterial[3] effects. These effects are mainly attributed to antioxidative, i.e., radical scavenging, activity.[4,5] We have reported that tea percolate and the component catechins have a strongly protective effect on radiation-induced scission of DNA that was attributed to the activity to scavenge the hydroxyl radical ($HO^{\bullet}$) produced by the decomposition of water molecules surrounding the DNA.[6−8]

Catechin is a group of polyphenols, and most polyphenols show radical-scavenging activity. A phenolic hydroxyl group (abbreviated as ϕ-OH) is considered the reactive point for the scavenging. However, a polyphenol has multiple ϕ-OHs, and therefore, it is not clear which ϕ-OH actually reacts. In addition, highly reactive radicals such as $HO^{\bullet}$ have the possibility of making an adduct to a double bond as in the case of the DNA base thymine. However, a polyphenol has multiple double bonds. Therefore, there are many possibilities for the reaction to scavenge radicals.

A polyphenol molecule changes into a radical when it reacts with $HO^{\bullet}$ in any reaction. Therefore, it can be expected that the reaction mechanism will be clarified by an analysis of the ESR spectrum of this polyphenol radical. However, the radicals usually have short lifetimes in aqueous solutions, and their esr spectra are difficult to measure by the conventional methods. We used a dielectric mixing resonator (DMR) to measure the spectrum of the 2-deoxy-D-ribose radical generated by reaction with the $HO^{\bullet}$.[9] The DMR has a high sensitivity and is relevant for the study of radicals derived from samples that cannot be obtained in large amounts, such as biological materials.

In this paper, we report the ESR spectra, which were measured using a DMR, of the polyphenol (catechol and gallic acid, which are thought to be model compounds for the partial structure of tea catechins) radicals formed by reaction with $HO^{\bullet}$ and their spectral simulation based on the Bloch equation. The simulated spectra were compared with the spectra of the radicals formed during autoxidation.

Experimental Section

Materials. As a $HO^{\bullet}$-generating system, the reaction between Ti^{3+} and H_2O_2 was used. The $HO^{\bullet}$ is generated by the following reaction

$$Ti^{3+} + H_2O_2 \rightarrow Ti^{4+} + OH- + HO^{\bullet} \qquad (1)$$

Ti^{3+} is very unstable in air and easily oxidized to Ti^{4+} by dissolved oxygen, so $TiCl_3$ in dilute HCl solution, commercially available from Wako Pure Chemical Co., Ltd., was used. Catechol and gallic acid were also purchased from Wako. Other chemicals were of guaranteed grade. Two aqueous solutions were prepared: Solution A contained $TiCl_3$ (1.0×10^{-2} M), H_2SO_4 (1.9×10^{-1} M), and the reactant (catechol or gallic acid, 1×10^{-1} M). Solution B contained H_2O_2 (8.0×10^{-2} M) and H_2SO_4 (1.9×10^{-1} M). These solutions were bubbled with N_2 gas to evacuate the dissolved oxygen just before use and were sucked into 25-mL syringes. In the case of autoxidation experiments, solution A was an aqueous solution of the polyphenol (1×10^{-3} M), and solution B was an aqueous NaOH (1×10^{-1} M) solution, with solution B being air-bubbled to saturate it with the oxygen necessary for autoxidation.

Method. Details on the DMR (Bruker, ER4117D-MVT) were explained in a previous paper.[9] Syringes were set on a syringe pump, and the two solutions were flowed into the mixing chamber at a total solution flow rate of 30 mL/min(the rate of each solution is one-half of this value). In the case of autoxidation, the flow rate was lowered to 10 mL/min because

* To whom correspondence should be addressed. Tel./Fax: +81-54-264-5784. E-mail: yoshioka@smail.u-shizuoka-ken.ac.jp.
† Institute for Environmental Sciences, University of Shizuoka.
‡ Shizuoka University.
§ School of Administration and Informatics, University of Shizuoka.

10.1021/jp021987p CCC: $25.00
Published on Web 01/30/2003

of the low reaction rate. ESR spectra were measured by a Bruker EMX spectrometer at room temperature with the following conditions: frequency, 9.6512 GHz; center field, 344.0 mT; sweep width, 2.5 mT; modulation frequency, 100 kHz; modulation widths, 0.063 mT (HO•) and 0.020 mT (autoxidation); number of measuring points, 512; conversion time, 40 ms; sweep time, 21 s; power, 8 mW.

Theory

Assuming that a group of spins exists in two states (A and B) and that each spin exchanges positions between them, the changes in magnetization of both states ($\hat{M}_A$ and $\hat{M}_B$) are expressed by the following Bloch equations[10]

$$\begin{aligned} d\hat{M}_A/dt + i(\hat{\omega}_A - \omega)\hat{M}_A + P_{AB}\hat{M}_A - P_{BA}\hat{M}_B = if_A(\gamma H_1 M_0) \\ d\hat{M}_B/dt + i(\hat{\omega}_B - \omega)\hat{M}_B + P_{BA}\hat{M}_B - P_{AB}\hat{M}_A = if_B(\gamma H_1 M_0) \end{aligned} \quad (2)$$

Here, $\hat{M}_A$ is the magnetization of spins in state A; $\hat{M}_B$ is the magnetization of spins in state B; ω is the angular frequency, with $\hat{\omega}_A = \omega_{0,A} - i/T_{2,A}$ and $\hat{\omega}_B = \omega_{0,B} - i/T_{2,B}$; $\omega_{0,A}$ and $\omega_{0,B}$ are the centers of the absorption lines of the A and B states, respectively; $T_{2,A}$ and $T_{2,B}$ are the spin−spin relaxation times of spins A and B, respectively, with $1/T_2$ related to the original line width (ΔW) via $\Delta W = 2/3^{1/2}T_2$; f_A and f_B are the fractions of spins occupying A and B states, respectively; P_{AB} and P_{BA} are the transition rate constants from A to B and from B to A, respectively; γ is the gyromagnetic ratio; H_1 is the amplitude of the microwave; M_0 is the Z component of the total magnetization; and i is the imaginary unit.

At the stationary state, $d\hat{M}_A/dt = d\hat{M}_B/dt = 0$, simultaneous linear eq 1 is solved, and the total magnetization M is given by

$$\begin{aligned} \hat{M} &= \hat{M}_A + \hat{M}_B \\ &= -\gamma H_1 M_0[f_A(\omega - \hat{\omega}_B) + f_B(\omega - \hat{\omega}_A) + i(P_{AB} + P_{BA})]/ \\ &\quad \{[(\omega - \hat{\omega}_A) + iP_{AB}][(\omega - \hat{\omega}_B) + iP_{BA}] + P_{AB}P_{BA}\} \end{aligned} \quad (3)$$

The imaginary part of M expresses the line shape of the spectra. This equation can also be used to simulate the ESR spectra of radicals that interconvert between two limiting structures such as the catechol radical.

In the case that a group of spins exists in three states (A, B, and C) and each spin exchanges positions among them, eqs 2 are is changed as follows

$$\begin{aligned} d\hat{M}_A/dt + i(\hat{\omega}_A - \omega)\hat{M}_A + P_{AB}\hat{M}_A + P_{AC}\hat{M}_A - P_{BA}\hat{M}_B - \\ P_{CA}\hat{M}_C = if_A(\gamma H_1 M_0) \\ d\hat{M}_B/dt + i(\hat{\omega}_B - \omega)\hat{M}_B + P_{BA}\hat{M}_B + P_{BC}\hat{M}_B - P_{AB}\hat{M}_A - \\ P_{CB}\hat{M}_C = if_B(\gamma H_1 M_0) \\ d\hat{M}_C/dt + i(\hat{\omega}_C - \omega)\hat{M}_C + P_{CA}\hat{M}_C + P_{CB}\hat{M}_C - P_{AC}\hat{M}_A - \\ P_{BC}\hat{M}_B = if_C(\gamma H_1 M_0) \end{aligned} \quad (4)$$

At the stationary state, $d\hat{M}_A/dt = d\hat{M}_B/dt = d\hat{M}_C/dt = 0$, so simultaneous linear eqs 4 are solved using the following matrix equation, which is available for computer calculation. The total magnetization is then obtained as the sum of $\hat{M}_A$, $\hat{M}_B$, and $\hat{M}_C$.

$$\begin{pmatrix} [i(\hat{\omega}_A - \omega) + P_{AB} + P_{AC}] & -P_{BA} & -P_{CA} \\ -P_{AB} & [i(\hat{\omega}_B - \omega) + P_{BA} + P_{BC}] & -P_{CB} \\ -P_{AC} & -P_{BC} & [i(\hat{\omega}_C - \omega) + P_{CA} + P_{CB}] \end{pmatrix} \begin{pmatrix} \hat{M}_A \\ \hat{M}_B \\ \hat{M}_C \end{pmatrix} = i\gamma H_1 M_0 \begin{pmatrix} f_A \\ f_B \\ f_C \end{pmatrix} \quad (5)$$

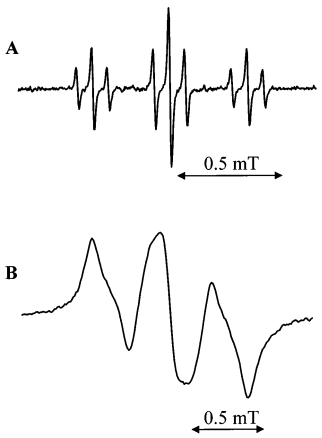

Figure 1. ESR spectra of the catechol radical formed (A) during autoxidation and (B) by reaction with HO•.

This equation was used for an analysis of the spectrum of the gallic acid radical. The simulations were performed using a revised Marquardt method,[11,12] in which variable parameters were first set as arbitrary values and then changed automatically in the direction that the difference between observed and calculated values becomes smaller. Finally, parameters that minimize the difference were obtained.

Results and Discussion

The ESR flow method was proposed more than 30 years ago, and ESR spectra of radicals derived from alcohols by reaction with HO• have been reported.[13−18] However, it has been rather difficult to measure those of polyphenols. This is because the lifetimes of polyphenol radicals are too short, and the radicals change into other species. We have shown that the reaction between a polyphenol molecule and a radical such as 1,1-diphenyl-2-picrylhydrazyl (DPPH) proceeds as a consecutive reaction and that one polyphenol molecule is able to scavenge more than 10 DPPH molecules in some cases.[19] Therefore, the polyphenol radical formed by the first step reacts rapidly with another DPPH molecule, which might be the origin of the short lifetime. On the other hand, polyphenols generate relatively stable, i.e., long-lived, radicals by autoxidation, and the ESR spectra can be measured easily.[20,21] The difference between these two cases seems mainly due to the difference in pH. That is, autoxidation is performed under strongly alkaline conditions in contrast to the reaction with HO•, where strongly acidic conditions must be applied. Therefore, we compared the ESR spectra of radicals formed by reaction with HO• with those measured during autoxidation.

Figure 1A shows the ESR spectrum measured during the autoxidation of catechol. It consists of a clearly resolved triple triplet, showing that two sets of equivalent protons are interacting with the unpaired electron. One of two ϕ-OHs of a catechol molecule is ionized in such alkaline solution, and therefore, electron transfer from ionized ϕ-OH to a dissolved oxygen occurs easily, as shown in Figure 2. The original anion changes into a neutral radical by this electron transfer, so this change induces ionization of a second ϕ-OH, resulting in the formation of an anion radical. As electron migration in a molecule is considered to be rapid enough compared to the following proton migration, the interconversion between these two limiting structures in the figure is also rapid, which makes the H_1 and H_2 protons equivalent; similarly, the H_3 and H_4

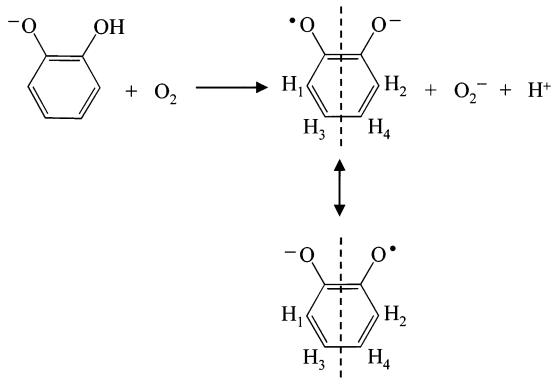

Figure 2. Scheme of catechol radical formation during autoxidation.

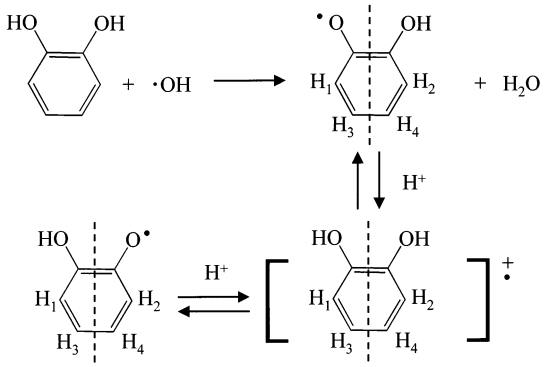

Figure 3. Mechanism of interconversion of the catechol radical between limiting structures in acidic conditions.

protons become equivalent. This is the reason the triple triplet spectrum was measured. However, it is not decisive which pair has a larger hyperfine splitting constant (hfsc).

Figure 1B shows the ESR spectrum of the radical formed by the reaction of catechol and HO•. A characteristic feature of this spectrum is that the lines are unusually broad compared with that measured in Figure 1A. The spectrum looks like a triplet, but each line of this pseudo-triplet has an unexplained line shape. We think that this strange spectrum can be explained as follows. As the solution is strongly acidic, catechol and the derived radical are not ionized. Catechol changes into a phenoxyl radical by the extraction of hydrogen atom with HO•, as shown in Figure 3. In contrast to the case in Figure 2, the unpaired electron cannot shift to another ϕ-OH, because this group is not ionized. If the radical retains this structure, the ESR spectrum must contain 16 lines because of the interaction with nonequivalent four protons. However, this cannot explain the line shape. We, therefore, considered that this radical structure is not stable and that the unpaired electron is actually able to move to another ϕ-OH. As a mechanism, it was assumed that the proton attaches to the radical under such acidic conditions, forming a catechol cation radical with the structure shown in the figure. Then, a proton is detached from the radical, but it is equally possible to detach from each ϕ-OH. Through this cation structure as an intermediate, an unpaired electron can move to another ϕ-OH. In other words, the radical changes between two limiting structures as shown in Figure 3. However, it might also be possible that the proton of the neighboring ϕ-OH jumps directly without the help of the solvent, but it is difficult to estimate the contribution of this mechanism. If this exchange rate is large enough, the H_1 and H_2 protons, as well as the H_3 and H_4 protons, become equivalent. This is the same case as in Figure 2, and a triple triplet spectrum will be obtained. However, the rate is not large enough because attachment and subsequent detachment of a proton are necessary for this interconversion. It can be expected that this exchange induces broadening of the absorption

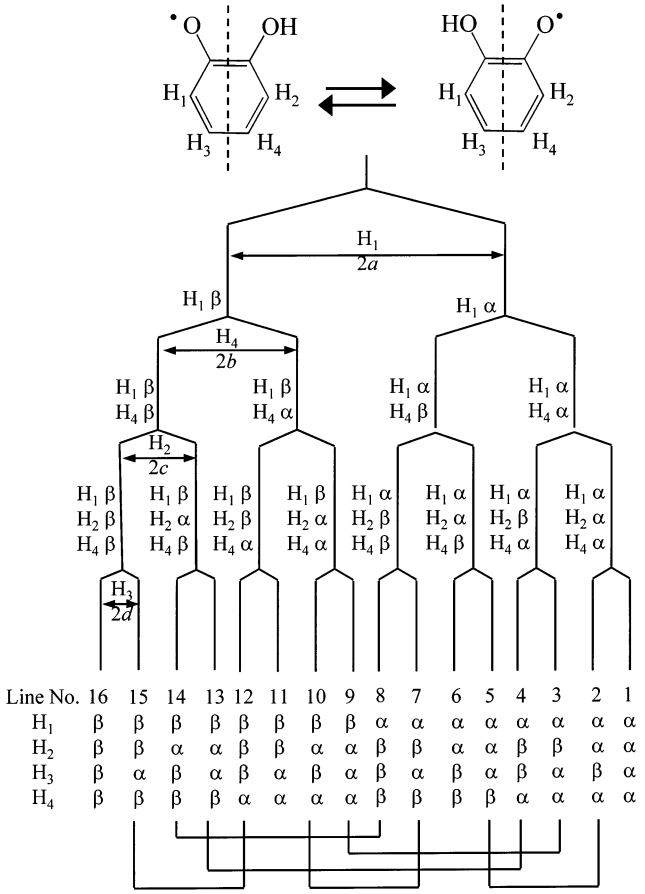

Figure 4. Schematic splitting diagram of the ESR spectra corresponding to the left limiting structure. α and β denote the spin states of each proton.

lines and that the spectrum changes largely depending on this exchange rate. Therefore, we tried a computer simulation setting the exchange rate as a parameter using the Bloch equation. As an important assumption for the simulation, it was considered that spin states of the interacting ring protons, H_1-H_4, do not change during the time of the exchange between the two structures. This means that longitudinal relaxation time of the protons is sufficiently longer than the reciprocal of the exchange rate. First, we considered the spectrum expected for one limiting structure. In the left limiting structure in Figure 4, the hfsc values of protons H_1-H_4 were set to be 2*a*, 2*c*, 2*d*, and 2*b*, respectively. We thought here that the hfsc's of the protons in the ortho and para positions would be larger than those in the meta positions and assumed an order of $a > b > c > d$ for ease in understanding the figure. However, this order of relative hfsc values does not affect the conclusion, and the exact result can be obtained even if the relation is changed. The expected spectrum contains 16 lines corresponding to the spin states of the four protons, as shown with the numbered lines in the figure. When interconversion occurs and the radical changes from the left to the right limiting structure, the spin states do not change, as stated above, but the hfsc values change between H_1 and H_2 and similarly between H_3 and H_4. Therefore, each ESR line must shift its position to another place. As the two limiting structures are mirror images, the change in the relations between the unpaired electron and the protons induced by the interconversion from the left to the right structure is equal to the case that the spin states were changed between H_1 and H_2 and also between H_3 and H_4 in the left limiting structure without the interconversion. As a result, for example, line 4 [$H_1(\alpha)$ $H_2(\beta)$ $H_3(\beta)$ $H_4(\alpha)$] shifts position to that of line 13 [$H_1(\beta)$ $H_2(\alpha)$ $H_3(\alpha)$ H_4-

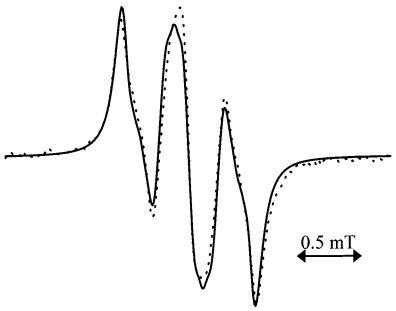

Figure 5. Comparison of simulated (solid) and measured (dotted) spectra of the catechol radical. The simulation was performed using the following values and those in Table 1: $P = 3.0 \times 10^5$ Hz, $\Delta W = 0.070$ mT.

TABLE 1: ω_0 Values of the Catechol Radical Calculated from hfsc's and the Best-Fit Values

line no.	from hfsc's	best-fit (mT)
1	$a+b+c+d$	0.49
2	$a+b+c-d$	0.43
3	$a+b-c+d$	0.37
4	$a+b-c-d$	0.30
5	$a-b+c+d$	0.16
6	$a-b+c-d$	0.09
7	$a-b-c+d$	0.03
8	$a-b-c-d$	−0.03
9	$-a+b+c+d$	0.03
10	$-a+b+c-d$	−0.03
11	$-a+b-c+d$	−0.09
12	$-a+b-c-d$	−0.16
13	$-a-b+c+d$	−0.30
14	$-a-b+c-d$	−0.37
15	$-a-b-c+d$	−0.43
16	$-a-b-c-d$	−0.49

(β)] by this interconversion. Simultaneously, the position of line 13 shifts to that of line 4. That is, the two lines exchange positions. The lines in which the pairs H_1 and H_2 and H_3 and H_4 have same spin states do not change positions. Accordingly, the 16 lines are divided into 4 unchangeable lines and 6 interacting sets of lines, as shown in the bottom of the figure. In each set, the positions of two lines shift, and the line widths change depending on the exchange rate, as expected from Bloch equation. The resulting spectrum is the superposition of the two sets of lines. We performed a computer simulation and compared the result with the measured spectrum. The ω_0 values of the lines could be calculated from the hfsc values and are listed in Table 1, where the center position of the spectrum is set to 0.

Figure 5 shows the experimental and best-fit spectra and the relatively good agreement between them. The parameters used for this calculation are shown in the legend and in Table 1. The dependence on the exchange rate is shown in Figure 6, in which the original line width was set to be smaller than the best-fit value to make the change clear. When $P \rightarrow 0$ and $P \rightarrow \infty$, the spectra exhibit 16 lines (two are overlapping) and 9 lines, and the shape changes depending on the P value. The order of hfsc values agreed with the expected one, suggesting that the obtained values were reasonable.

The ESR spectrum of the gallic acid radical formed by autoxidation is shown in Figure 7A. It is a simple triplet, showing that two protons are equivalent. A carboxyl group must be ionized in this case, but the ionization of the two ϕ-OHs is not clear. The unpaired electron locates mainly on the central oxygen atom as shown in the figure, so both ϕ-OHs must be ionized or nonionized simultaneously to be equivalent. We thought that the ionized state would be more probable in such strongly alkaline solution, meaning that the radical is a trivalent cation. As the pK_a value of the third ionization of pyrogallol,

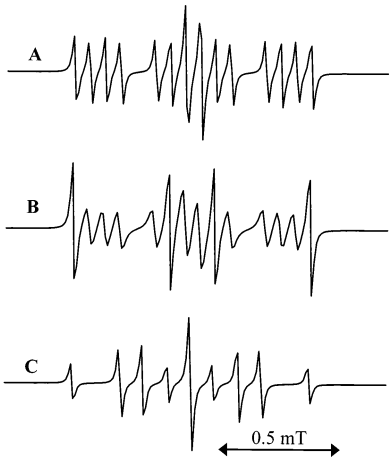

Figure 6. Dependence of the spectra of the catechol radical on the exchange rate. (A) $P = 0$ Hz, (B) $P = 3.0 \times 10^5$ Hz, (C) $P = \infty$ Hz; $\Delta W = 0.010$ mT.

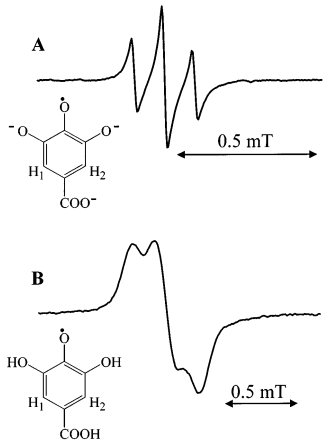

Figure 7. ESR spectra of the gallic acid radical formed (A) during autoxidation and (B) by reaction with HO•.

which contains three ϕ-OHs, was reported to be 14, showing that it is trivalent at pH's higher than 14, it is natural to consider that the gallic acid radical, which contains a carboxylic group and two ϕ-OHs, can be trivalent more easily than pyrogallol. In this case, the unpaired electron easily migrates in a molecule, and the equivalence of the two ring protons holds strictly.

Figure 7B shows the ESR spectrum of the radical formed by the reaction of gallic acid and HO•. The line is unusually broad compared with that of autoxidation as in the case of catechol. We found that dehydrogenation with HO• also occurred and that a neutral phenoxy radical was formed; this structure is shown in the figure. The unpaired electron might be able to move to another ϕ-OH through the same mechanism as for the catechol radical. Therefore, spectral simulations were also performed setting the interconversion rate as a parameter. The gallic acid radical takes the three limiting structures shown in Figure 8. In the central (m) structure, the two protons are equivalent and have the same hfsc value, $2a$, the spectrum being a triplet. In the left (l) structure, the protons are not equivalent, and the values are $2b$ (H_1) and $2c$ (H_2), resulting in a double doublet spectrum. The right structure is the mirror image of the left one; therefore, the hfsc values of H_1 and H_2 alternate, namely, $2c$ (H_1) and $2b$ (H_2). The spin states corresponding to each line are shown in the figure. The positions of the lines of the three structures corresponding to one of the four spin states were calculated from the hfsc values and are listed in Table 2. Simulations were performed assuming that the absorption line interconverts among these three positions and that the overall

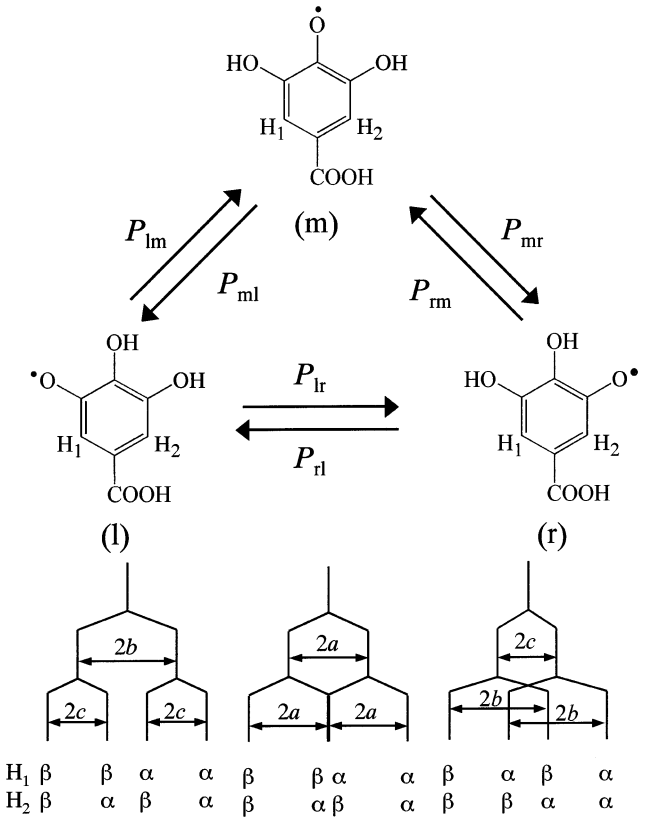

Figure 8. Schematic splitting diagram of the ESR spectra of the gallic acid radical corresponding to each limiting structure.

TABLE 2: ω_0 Values of the Gallic Acid Radical Calculated from hfsc's and the Best-Fit Values

spin state	from hfsc	best fit (mT)
$H_1(\alpha)\ H_2(\alpha)$	$\omega_{0,m} = 2a$	0.12
	$\omega_{0,l} = b + c$	0.20
	$\omega_{0,r} = b + c$	0.20
$H_1(\alpha)\ H_2(\beta)$	$\omega_{0,m} = 0$	0
	$\omega_{0,l} = b - c$	−0.05
	$\omega_{0,r} = -b + c$	0.05
$H_1(\beta)\ H_2(\alpha)$	$\omega_{0,m} = 0$	0
	$\omega_{0,l} = -b + c$	0.05
	$\omega_{0,r} = b - c$	−0.05
$H_1(\beta)\ H_2(\beta)$	$\omega_{0,m} = -2a$	−0.12
	$\omega_{0,l} = -b - c$	−0.20
	$\omega_{0,r} = -b - c$	−0.20

spectrum is the superposition of four sets of these spectra. In this system, the exchange rate, P_{ml}, is not the same in the reverse direction, P_{lm}. However, the relations $P_{ml} = P_{mr}$, $P_{lm} = P_{rm}$, and $P_{lr} = P_{rl}$ hold from their symmetric relations. The fractions taking each structures, f_m, f_l, and f_r, are not equal, but the following relations must hold at the stationary spin states

$$f_l = f_r$$

$$f_c + f_l + f_r = 1$$

$$f_m(P_{ml} + P_{mr}) = f_l P_{lm} + f_r P_{rm} \qquad (6)$$

Accordingly, P_{ml}, P_{lm}, and P_{lr} were chosen as independent variables, and the other P and f values were calculated using above relations.

Figure 9 shows the experimental and the best-fit spectra, the parameters being shown in the legend and in Table 2. The dependence on the exchange rate is shown in Figure 10, in which the original line width was set to be smaller than the best-fit

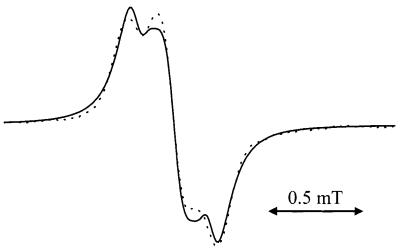

Figure 9. Comparison of simulated (solid) and measured (dotted) spectra of the gallic acid radical. The simulation was performed using the following values and those in Table 2: $P_{ml} = 6.2 \times 10^5$ Hz, $P_{lm} = 1.9 \times 10^5$ Hz, $P_{lr} = 3.2 \times 10^5$ Hz, $\Delta W = 0.084$ mT.

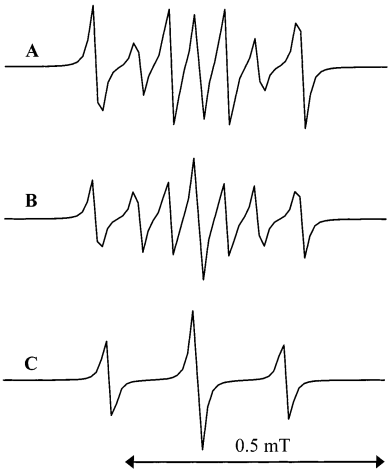

Figure 10. Dependence of the spectra of the gallic acid radical on the exchange rate. (A) $P_{ml} = 0$ Hz, $P_{lm} = 0$ Hz, $P_{lr} = 0$ Hz; (B) $P_{ml} = 6.2 \times 10^5$ Hz, $P_{lm} = 1.9 \times 10^5$ Hz, $P_{lr} = 3.2 \times 10^5$ Hz; (C) $P_{ml} = \infty$ Hz, $P_{lm} = \infty$ Hz, $P_{lr} = \infty$ Hz; $\Delta W = 0.010$ mT.

value to make the change clear. When $P \rightarrow 0$ and $P \rightarrow \infty$, the spectra contain 7 lines and a triplet, and the shape changes depending on the P value.

The exchange rates obtained from the simulation were in the range of 10^5−10^6 Hz. In this treatment, we assumed that the time of existence as an intermediate, cation radical, is very short. Therefore, the exchange rate is determined by the second-order rate constant of the association reaction between a proton and the radical. Assuming that $[H^+] = 10^{-1}$ M, the constants are in the range of 10^6−10^7 M^{-1} s^{-1}. The second-order rate constants of the association reactions between a proton and anions are in the range of 10^7−10^{11} M^{-1} s^{-1}, widely distributed depending on the structure of anions. The values obtained here seem to be reasonable enough, because neutral radicals might have lower reactivities with a proton than anions.

From these results and the discussion, it was shown that our conception was reasonable. That is, polyphenol radicals formed by reaction with HO• are phenoxy radicals, and their conformations interconvert at finite rates between the limiting structures. In other words, polyphenols scavenge HO• using a ϕ-OH, as usually expected. However, it might be impossible to determine which ϕ-OH is used from the ESR spectra because the radical is changing among a few structures.

References and Notes

(1) Wang, Z. Y.; Khan, W. A.; Bickers, D. R.; Mukhtar, H. *Carcinogenesis* **1989**, *10*, 411−415.

(2) Lee, I. P.; Kim Y. H.; Kang, M. H.; Roberts, C.; Shim, J. S.; Roh, J. K. *J. Cell. Biochem. Suppl.* **1997**, *27*, 68−75.

(3) Shetty, M.; Subbannayya, K.; Shivananda, P. G. *J. Commun. Dis.* **1994**, *26*, 147−150.

(4) Guo, Q.; Zhao, B.; Li, M.; Shen, S.; Xin, W. *Biochim. Biophys. Acta* **1996**, *1304*, 210−222.

(5) Nanjo, F.; Mori, M.; Goto, K.; Hara, Y. *Biosci. Biotechnol. Biochem.* **1999**, *63*, 1621−1623.
(6) Yoshioka, H.; Akai, G.; Yoshinaga, K.; Hasegawa, K.; Yoshioka, H. *Biosci. Biotechnol. Biochem.* **1996**, *60*, 117−119.
(7) Yoshioka, H.; Kurosaki, H.; Yoshinaga, K.; Saito, K.; Yoshioka, H. *Biosci. Biotechnol. Biochem.* **1997**, *61*, 1560−1563.
(8) Yoshioka, H.; Yoshioka, H. *Recent Res. Dev. Agric. Biol. Chem.* **1998**, *2*, 419−427.
(9) Ohashi, Y.; Yoshioka, H.; Yoshioka, H. *Biosci. Biotechnol. Biochem*. **2002**, *66*, 847−852.
(10) Carrington, A.; McLachlan, A. D. *Introduction to Magnetic Resonance with Applications to Chemistry and Chemical Physics*; Harper & Row: New York, 1967; Chapter 12.
(11) Marquardt, D. W. *SIAM J. Appl. Math*. 1963, *11*, 431−441.
(12) Osborne, M. R. *J. Aust. Math. Soc.* **1976**, *19*, 343−357.
(13) Dixon, W. T.; Norman, R. O. C. *J. Chem. Soc.* **1963**, 3119−3124.
(14) Shiga, T. *J. Phys. Chem.* **1965**, *69*, 3805−3814.
(15) Norman, R. O. C.; Pritchett, R. J. *J. Chem. Soc. B* **1967**, 1329−1332.
(16) Gilbert, B. C.; King, D. M.; Thomas, B. *J. Chem. Soc., Perkin Trans. 2* **1980**, 1821−1827.
(17) Gilbert, B. C.; King, D. M.; Thomas, B. *J. Chem. Soc., Perkin Trans. 2* **1981**, 1186−1199.
(18) Gilbert, B. C.; King, D. M.; Thomas, B. *J. Chem. Soc., Perkin Trans. 2* **1983**, 675−683.
(19) Senba, Y.; Nishishita, T.; Saito, K.; Yoshioka, H.; Yoshioka. H. *Chem. Pharm. Bull.* **1999**, *47*, 1369−1374.
(20) Yoshioka, H.; Sugiura, K.; Kawahara, R.; Fujita, T.; Makino, M.; Kamiya, M.; Tsuyumu, S. *Agric. Biol. Chem*. **1991**, 2717−2723.
(21) Yoshida, T.; Mori, K.; Hatano, T.; Okumura, T.; Uehara I.; Komagoe, K.; Fujita, Y.; Okuda, T. *Chem. Pharm. Bull.* **1989**, *37*, 1919−1921.